Extension of the tip excitation technique to the rotational compliance measurement of curved structures

L. Cheng and Y. C. Qu
Department of Mechanical Engineering, Université Laval, Québec, Québec G1K 7P4, Canada

(Received 18 December 1995; accepted for publication 20 September 1996)

The present paper presents an extension of the so-called tip excitation technique for measuring the rotational compliance of curved structures. On the basis of the original form of the technique, developed for attached plane structures, the technique is improved to take into account the presence of the in-plane vibration and the rigid motion. Two derivatives of the technique are developed: the first one using two accelerometers allows a more accurate indication of rotational response, thus providing a good accuracy in middle frequency range; the second one using double excitation effectively eliminates the in-plane force excitation, thus providing an excellent measurement accuracy at both low and middle frequencies. Numerical simulations using finite element modeling are performed to analyze different parameters affecting the performance of the technique. Experimental validations are then reported. It is shown that the technique is successfully extended to curved structures while retaining the advantages of the original version of the method in terms of its simplicity and its capacity for mass loading compensations. © *1997 Acoustical Society of America.* [S0001-4966(97)00902-8]

PACS numbers: 43.40.Yq, 43.40.At [CBB]

INTRODUCTION

Mechanical compliance and mobility concepts have become one of the standard tools to characterize the dynamic behavior of structures. Their wide application demands that both theoretical and experimental techniques be developed.[1] Compared to the translational compliance, the rotational compliance measurement is much more difficult due to the access to the quantities related to the rotational degrees of freedom. Two major obstacles to overcome include the acquisition of rotational responses and the production of a moment excitation.[2,3] The situation is even more critical when one handles light thin-walled structures, since any measuring device physically connected to the system will tend to affect the dynamics of the original structure.

Due to these difficulties, there exists only a very short list of references dealing with the rotational compliance or mobility measurement, as reported by some very recent works.[4–7] The classical approach is the double-exciter method, using a pair of dynamic exciters operated in phase opposition to provide moment excitation via a simple lever. Since its development, it remains the method that is mostly used. Effort has been made recently to improve the method by taking into account the loading effects of the exciter.[4,5] However, main difficulties related to the method lie in the production of a perfect phase match between two exciters to ensure a perfect phase opposition. In addition to that, the quality of the excitation can still be poor due to the mass introduced by the exciting configuration.

As an attempt to address the rotational measurement problem, a so-called tip excitation technique (TET), was recently proposed.[6,7] In this approach, a beamlike tip is used to transfer a force excitation into a torque and the rotational response into a translational one, thus converting a rotational measurement problem into a translational one, permitting the use of conventional apparatus. Using a single force exciter or an impact hammer, the TET avoids the matching difficulties encountered in the double-exciter method. Also, a dynamic analysis of the tip motion allows one to eliminate the mass effect of the tip on the structure to be measured. On the basis of a cantilevered rectangular plate, the technique was numerically and experimentally assessed, showing that the TET is feasible to use in low- and middle-frequency ranges for plane structures. However, the hypotheses made in the development of the technique restrain its application only to attached plane structures, whose in-plane motion can be mostly neglected compared with the flexible motion. This technique will hereafter be called the original TET.

As a continuation of the previous work, this paper first discusses the applicability of the original TET to curved structures that may involve significant in-plane motion. The so-called in-plane motion, due to the curvature or free boundaries, represents the movement of the measuring point in the tangential plane of the structure. After a brief review of the technique, the original TET without any modification is first applied to a series of curved panels with varying curvatures. Curvature effects are then analyzed, leading to some modifications of the technique. Two alternatives using two accelerometers with single or double excitations are further investigated. The modified TET using two accelerometers with single excitation eliminates unwanted translational response to enhance the accuracy of the rotation measurement, while the modified TET with double excitation eliminates effects of the in-plane force excitation. Finally, experiments using a free panel are carried out to assess the technique. Both numerical and experimental results illustrate the performance of each version of the technique, as well as the applicability of each.

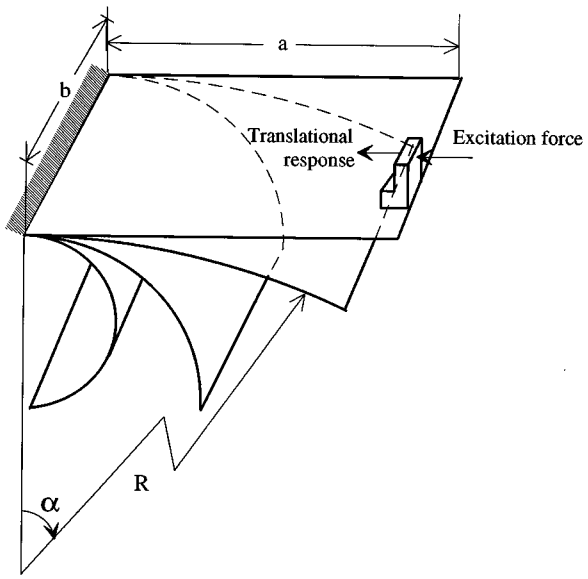

FIG. 1. Curved panels with various curvatures.

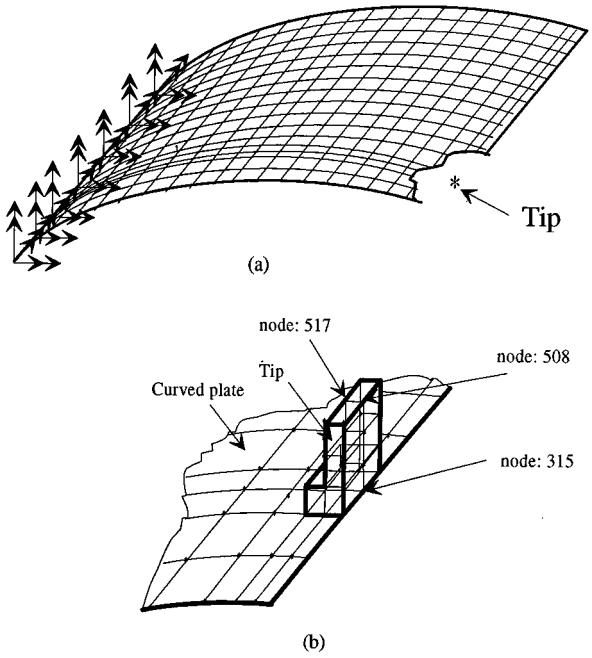

FIG. 2. FEA mesh of a typical curved panel-tip combination.

I. REVIEW OF THE TECHNIQUE AND DESCRIPTION OF THE PROCEDURE

The TET consists of attaching a small beamlike tip to a point on the structure where the rotational compliance has to be evaluated as illustrated in Fig. 1. For illustrating purpose, assume that the rotational compliance about the free edge is under investigation. By applying a driving force at the tip, an excitation moment is produced at the tip–structure intersection. In addition to that, the tip's motion provides information about the rotation undergone by the structure. On the basis of simultaneous measurements of the exciting force and the resulting acceleration, the rotational compliance of the structure is to be derived. A rigid body dynamic analysis of the tip is then performed, taking into account the coupling at the intersection of the structure and the tip, resulting in analytical formulas for rotational compliance. This procedure yields the following expression for both the compliance amplitude A_{cr} and the phase angle ϕ_{cr}:

$$A_{\mathrm{cr}}=\frac{1}{\omega^2}\Big/\sqrt{\left(\frac{K}{T}\right)^2-2I_{yy}\frac{K}{T}\cos\phi_a+I_{yy}^2}, \tag{1}$$

$$\tan\phi_{\mathrm{cr}}=\frac{-I_{yy}\sin\phi_a}{I_{yy}-(K/T)\cos\phi_a}, \tag{2}$$

where I_{yy} is the total effective moment of inertia of the tip about the rotation axis, passing through the contact region between the tip and the panel and parallel to the panel's free edge in the specific configuration shown in Fig. 1; T and ϕ_a are, respectively, the amplitude and the phase angle of the translational accelerance (acceleration/force) measured on the tip; and K is a geometric parameter which depends on the position of the excitation and that of the acceleration response. It is worth noting that the above expressions have proven to be effective in partially eliminating the inertial effects of the tip on the rotational compliance. However, these analytical relations were obtained on the basis of several hypotheses and simplifications, taking advantage of the fact that the structure under investigation is an attached plane panel so that all quantities relating to the in-plane motion had been neglected.[6] This should certainly be the main obstacle to remove regarding the extension of the technique to general curved structures.

In order to investigate the applicability of the TET to curved structures, a series of curved panels with varying curvatures are chosen as illustrated in Fig. 1. Taking a plane panel as a starting point, the panel is then bent so that the sector angle α varies from 0° (plane panel) to 180° (semicylindrical shell), while keeping all other dimensions and characteristics unchanged (length $a=400$ mm; width $b=300$ mm; thickness $h=3$ mm; density $\rho=7820.0$ kg/m^3; Young's modulus $E=2.068E+11$ N/m^2 and Poisson ratio $\mu=0.30$). An aluminum tip is used to estimate the rotational compliance of the panels at a point 5 cm from the corner along the free straight edge. The tip is designed according to the principles previously developed[6] and all its dimensions (as indicated in Fig. 5). As to the boundary conditions of the panels at the left end, either clamped edge or a free edge is to be investigated in the analyses.

Finite element analyses (FEA) using I-DEAS software are performed for the curved panels and the curved panel–tip combinations. For the former, the angular response of the panel under a pure moment excitation is calculated to provide the *expected results* of the rotational compliance. For the latter, assuming a unit force excitation on the tip, FEA calculates the quantities that should be measured in practice. The rotational compliance is then calculated using the derived compliance formula [Eqs. (1) and (2) for the original TET or other corresponding expressions that will be derived later when the TET is modified]. The results obtained are referred to as the *simulated results*.

The mesh of the curved panel–tip combination is illustrated in Fig. 2. The panel is discretized into 340 linear thin

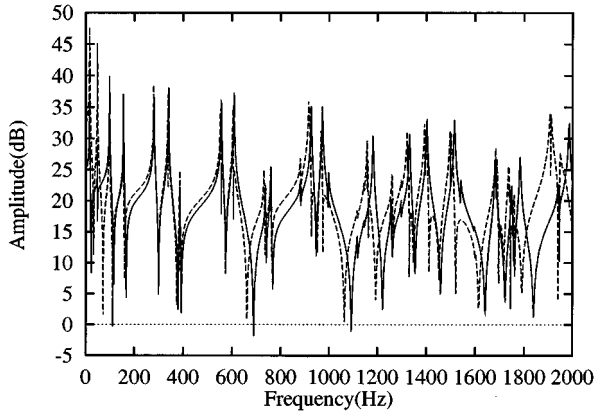

FIG. 3. Comparison of the rotational compliance of the panel with $\alpha=30°$. Original TET. Expected results: (———); simulated results: (------).

shell elements and the tip is divided into 8 linear solid elements. Convergence tests were made to ensure that the number of elements used was sufficient for the frequency range considered in this paper. For the curved panel, an exciting moment is applied at node 315 where the rotational compliance is to be evaluated. For the panel–tip combination, an exciting force is applied at node 508 and the translational acceleration at node 517 is calculated on the tip, allowing the estimation of the rotational compliance at node 315 on the curved panel.

II. DIRECT APPLICATION OF THE ORIGINAL TET

The original TET previously established is first applied to the curved panels. Figures 3 and 4 show the amplitude of the rotational compliance of the curved panels with two different sector angles: $\alpha=30°$ and $\alpha=180°$, respectively. Curves corresponding to the two cases are plotted for different frequency ranges so that a compatible amount of modes are included. The results are expressed in dB referencing to $1.0E-5$ rad/N m $[10\log(A_{cr}/1.0E-5)]$. In both cases, the *simulated results* are compared with the *expected results*. It can be seen that although the two panels exhibit different dynamic characteristics, the overall tendency in terms of compliance estimation accuracy is quite similar. Generally speaking, the amplitude level discrepancy varies with the

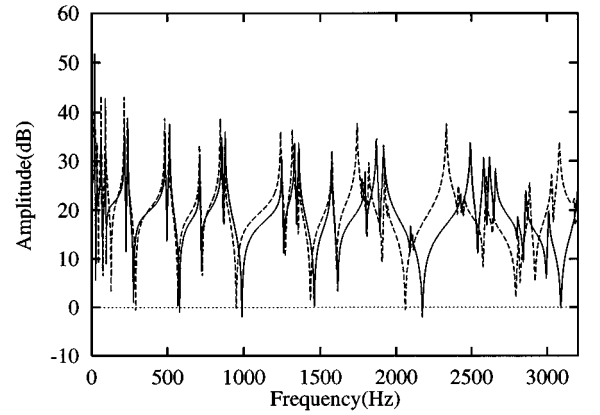

FIG. 4. Comparison of the rotational compliance of the panel with $\alpha=180°$. Original TET. Expected results: (———); simulated results: (------).

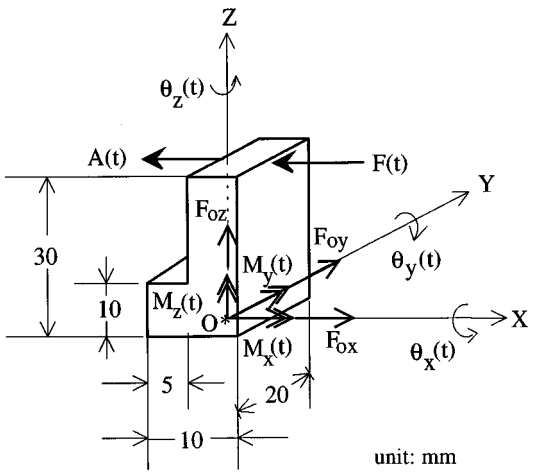

FIG. 5. Dynamic model of the tip.

frequency zone and the curvature. When the curvature becomes greater, the discrepancy seems to increase. More specifically, we notice a very bad accuracy of the technique at low frequencies involving the first 3–4 modes (zone A). In fact, both configurations present a discrepancy oscillating around 10 dB between the expected results and the simulated ones. The rigid motion of the tip in the excitation direction is believed to be the most responsible for this discrepancy, since a single accelerometer is no longer sufficient to accurately indicate the rotational response of the structure. At the middle-frequency range up to 10 modes (zone B), the technique seems to work reasonably well. With the increase of the frequency (zone C), we notice a degradation of the technique, which was also observed in the case of plane structures, mainly resulting from the coupling between the tip and the tested structure. It should be noted that the existence of the three zones is quite obvious while the dividing line between each zone may vary from structure to structure. These results seem to indicate that the original TET can be directly used for the curved structures only in the middle-frequency range (zone B). The advantage consists in its simplicity since only one accelerometer and a single excitation are required. However, modifications must be made to improve the technique at low frequencies.

III. MODIFIED TET USING TWO ACCELEROMETERS

The first step to improve the technique consists in using two accelerometers to get a more accurate indication of the rotational response of the curved structures. To this end, a dynamic analysis is performed for the tip by considering it as a rigid body. Figure 5 illustrates all possible existing forces and moments applied on the tip through the reaction of the curved structure. Note that all these quantities are decomposed into components in three directions in the established coordinate system. The frame is set in a way that the Z axis passes through the mass center of the tip. The complete equation of motion related to the rotation about Y axis is as follows:[8]

$$m_t(a_{ox}\overline{z}-a_{oz}\overline{x})+I_{yy}\ddot{\theta}_y+(I_{xx}-I_{zz})\dot{\theta}_x\dot{\theta}_z$$
$$+I_{yz}(\dot{\theta}_y\dot{\theta}_x-\ddot{\theta}_z)-I_{xy}(\dot{\theta}_y\dot{\theta}_z+\ddot{\theta}_x)+I_{xz}(\dot{\theta}_x^2-\dot{\theta}_z^2)$$
$$=M_y(t)-h_fF(t), \tag{3}$$

where I_{xx}, I_{yy}, I_{zz}, I_{yz}, I_{xy}, I_{xz} are the moments of inertia of tip with respect to different axes; $\theta_x, \theta_y, \theta_z$ the angular displacements about the X, Y, Z axes, respectively; $\overline{x}$, $\overline{z}$, $\overline{y}$ the coordinates of the mass center of the tip in O-XYZ frame; a_{Ox}, a_{Oz} the two acceleration components of the tip at its base along X and Z axis; m_t the mass of the tip; $M_y(t)$ the reacting moment and h_f the distance between the applied force $F(t)$ and the X axis.

Due to the symmetric geometry of the tip about XOZ plane, $I_{xy}=I_{yz}=0$. Equation (1) becomes

$$m_t(a_{ox}\overline{z}-a_{oz}\overline{x})+I_{yy}\ddot{\theta}_y+(I_{xx}-I_{zz})\dot{\theta}_x\dot{\theta}_z+I_{xz}(\dot{\theta}_x^2-\dot{\theta}_z^2)$$
$$=M_y(t)-h_fF(t). \tag{4}$$

In the above equation, the last two terms at the left-hand side represent the coupling between the rotation about Y and X axis, and the one between Y and Z axis. Compared with other terms in the equation, these two terms are higher order terms for small amplitude vibration and can therefore be neglected. Additionally, the fact that the Z axis passes through the mass center of the tip yields $\overline{x}=0$ and $\overline{y}=0$. Hence Eq. (4) is simplified as

$$m_ta_{ox}(t)\overline{z}+I_{yy}\ddot{\theta}_y(t)=M_y(t)-h_fF(t). \tag{5}$$

For the plane structure, considering the high stiffness in the in-plane direction, the first term at the left-hand side can be neglected since the in-plane acceleration component a_{ox} is much smaller than all other quantities. For curved panels however, it should be kept, which demands the use of another accelerometer along the X axis.

Assuming a harmonic excitation, the reacting moment at the panel-tip intersection can be derived from Eq. (5) as follows:

$$M_y(t)=(h_fF_0-I_{yy}\theta_0\omega^2e^{j\phi_\theta}+m_t\overline{zA}_{Ox}e^{j\phi_{Ox}})e^{j\omega t}, \tag{6}$$

where F_0 is the amplitude of exciting force; ω the angular frequency; θ_0 and ϕ_θ the amplitude and phase angle of the angular displacement response; A_{Ox} and ϕ_{Ox} the amplitude and phase angle of the linear acceleration at the base of the tip along X axis.

For a point on the tip, the translational acceleration in the X direction can be written as[8]

$$a_x(t)=a_{Ox}(t)+\ddot{x}-x(\Omega_y^2+\Omega_z^2)+y(\Omega_x\Omega_y-\dot{\Omega}_z)$$
$$+z(\Omega_x\Omega_z+\dot{\Omega}_y)+2(\dot{z}\Omega_y-\dot{y}\Omega_z), \tag{7}$$

in which Ω stands for the angular velocities with respect to different axes. In principle, the translational acceleration depends not only on the rotation about X, Y, and Z axes but also the translational acceleration at the origin. In the present case where the point of interest is a fixed point on the tip with respect to the reference frame, the coordinates of the point of interest are constants ($x\approx0$ due to the small thickness of the tip, $y=0$, $z=h_a$). Hence, $\dot{x}=\dot{y}=\dot{z}=0$, $\ddot{x}=\ddot{y}=\ddot{z}=0$. By neglecting the higher order terms and replacing $\dot{\Omega}_y$ by $\ddot{\theta}_y$, one obtains the following expression:

$$a_x(t)-a_{Ox}(t)=h_a\ddot{\theta}_y(t). \tag{8}$$

Assuming $\Delta a_x(t)=a_x(t)-a_{Ox}(t)=\Delta A_xe^{j(\omega t+\Delta\phi_a)}$, Eq. (8) becomes

$$\theta_0\omega^2=\frac{\Delta A_x}{h_a}, \tag{9}$$

where ΔA_x stands for the amplitude of the difference between $a_x(t)$ and $a_{Ox}(t)$, and h_a is the distance between the X axis and the point of measurement of acceleration.

According to the definition of the rotational compliance and, one can derive the rotational compliance $CR=\theta_y/M_y$ under complex forms:

$$\mathrm{CR}=\frac{1}{\omega^2}\Big/\left(I_{yy}-\frac{K}{\Delta T}e^{-j\Delta\phi_a}-K_ce^{j(\phi_{Ox}-\Delta\phi_a)}\right), \tag{10}$$

where $K=h_fh_a$ is a geometric parameter; $\Delta T=\Delta A_x/F_O$, and $K_c=m_t\overline{zA}_{Ox}(h_a/\Delta A_x)$.

From Eq. (10), the rotational compliance can be expressed in terms of amplitude A_{cr} and phase angle ϕ_{cr} as

$$A_{\mathrm{cr}}=\frac{1}{\omega^2}\Big/\sqrt{\left(\frac{K}{\Delta T}\right)^2-2I_{yy}\frac{K}{\Delta T}\cos\Delta\phi_a+I_{yy}^2+K_c^2+2K_c\frac{K}{\Delta T}\cos\phi_{Ox}-2I_{yy}K_c\cos(\phi_{Ox}-\Delta\phi_a)},$$

$$\tan\phi_{\mathrm{cr}}=-\frac{I_{yy}\sin\Delta\phi_a+K_c\sin(\phi_{Ox}-\Delta\phi_a)}{I_{yy}-(K/\Delta T)\cos\Delta\phi_a+K_c\cos(\phi_{Ox}-\Delta\phi_a)}. \tag{11}$$

Compared with the original TET using a single accelerometer expressed by Eqs. (1) and (2), the modified TET requires the use of two accelerometers situated respectively at the top and the base of the tip. By doing so, we hope to measure more accurately the rotation. Furthermore, the additional terms in Eq. (11) with respect to Eqs. (1) and (2) include the possible rigid motion of the tip along the X axis and therefore help to improve the performance of the added inertia compensation.

The modified TET using two accelerometers is applied to the two curved panels previously investigated. The simulated compliances are again compared with the expected re-

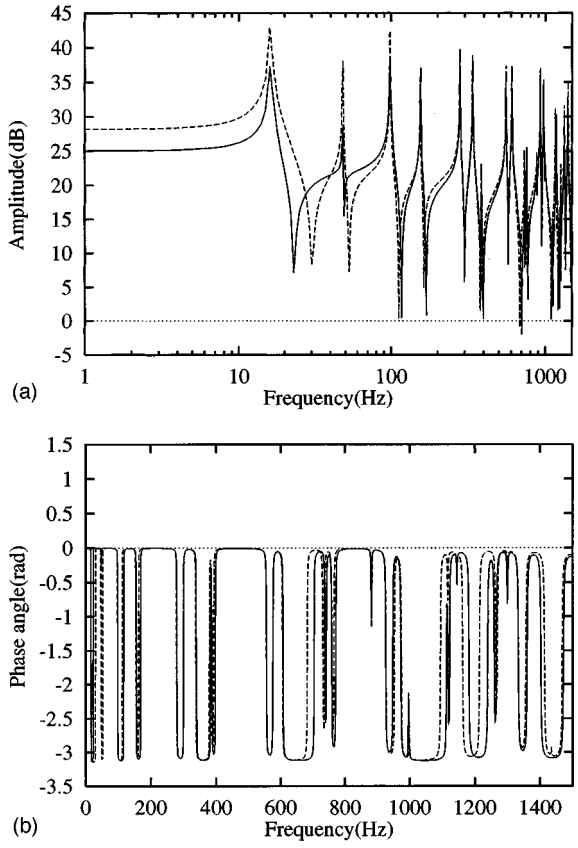

FIG. 6. Comparison of the rotational compliance of the panel with α=30°. Modified TET. Expected results: (———); simulated results: (------). (a) Amplitude; (b) phase angle.

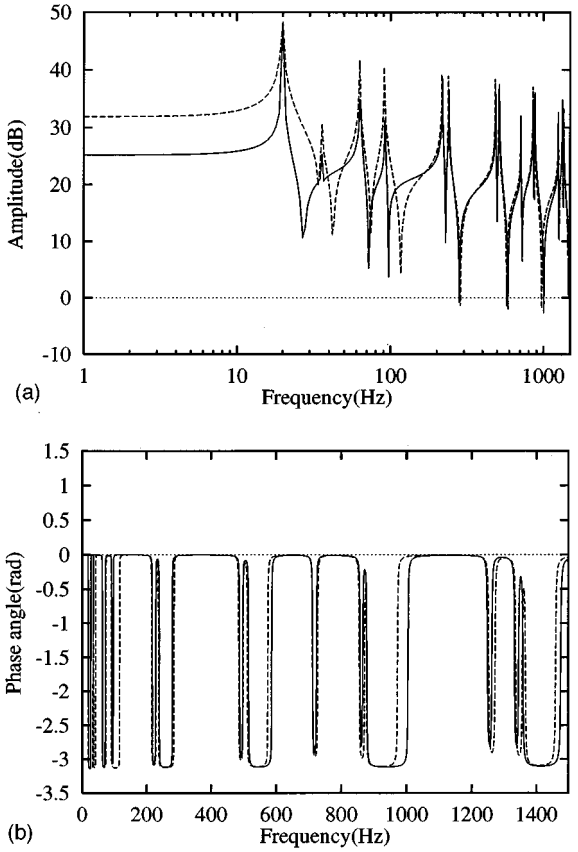

FIG. 7. Comparison of the rotational compliance of the panel with α=180°. Modified TET. Expected results: (———); simulated results: (------). (a) Amplitude; (b) phase angle.

sults for α=30° and α=180° in terms of amplitude and phase angle. The results are presented in Figs. 6(a), (b), 7(a), and (b). In order to better show the performance of the technique at the low-frequency range, the amplitude results are presented in a logarithm frequency scale. It can be seen that the modified TET greatly improves the accuracy of the simulated compliance in amplitude level and the resonance frequency. At very low frequencies, the 10-dB difference noticed previously with the original TET is reduced to some 3 and 7 dB for the 30° panel and 180° panel, respectively.

Before going to further improvement of the technique, we propose several indicators to quantify the errors due to the measurement technique. It is believed that the obtained results should be split out in terms of the modal response to make the conclusions more representative on one hand, and to cover a wider spectrum of panels on the other hand. To this end, the previous expected and simulated results were firstly decomposed into modal responses. Then the errors were calculated for each mode. Two indicators are then proposed to indicate the errors associated with resonance peak positions and the amplitude levels. Figure 8 illustrates two typical modal compliance curves corresponding to the simulated and expected results respectively. The two following indicators are used:

(1) *Amplitude error* relative to the compliance level: For a given mode i, it is defined as $A_s^i - A_e^i$, where A_s^i and A_e^i are, respectively, the average amplitude levels of the simulated and expected modal compliance over a band of 100 Hz around their own resonance frequencies f_s^i and f_e^i. Note that the average result is also expressed in dB. This parameter indicates how close the estimated compliance level is compared with the expected one.

(2) *Resonance frequency error* relative to the resonance frequency shift: For a given mode i, it is defined as $(f_s^i - f_e^i)/f_s^i$ in percentage, where f_s^i and f_e^i are, respectively, the resonance frequencies corresponding to the simulated and expected compliances. This parameter indicates how close the estimated natural frequency is compared with that of the single panel.

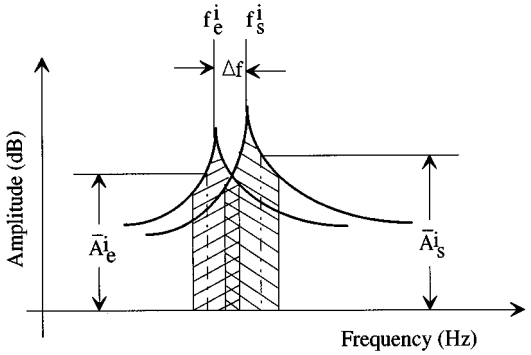

FIG. 8. Illustration of the error indicator definition in terms of modal compliance.

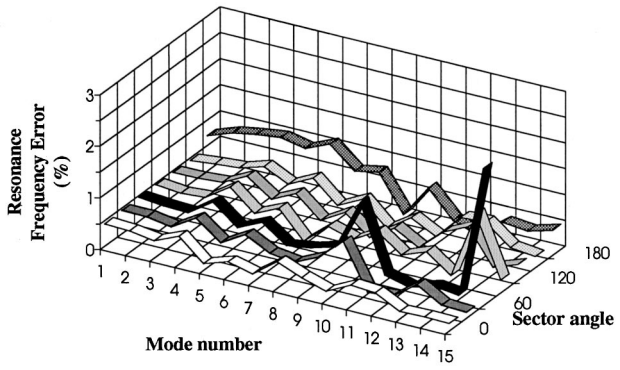

FIG. 9. Comparison of the resonance frequency error of modal response.

Using these definitions, the modified TET using two accelerometers is applied to panels with seven different curvatures (α=0°; 30°; 60°; 90°; 120°; 150°; and 180°). For each panel, the first 15 modes are investigated. The error results are presented in Figs. 9 and 10 showing, respectively, the variation of the amplitude error and that of the resonance frequency error versus the mode number and the sector angle. It can be seen from Fig. 9 that the technique seems to limit the resonance frequency shift to an acceptable level. In fact, for all panels, the resonance frequency error is usually less than 2% for all modes considered, indicating that the inertia effect due to the tip is well compensated. Figure 10 shows that the amplitude error associated with lower order modes increase with the curvature of the structure. Then the technique seems to work well before going into a zone of high order modes, where the error is somewhat amplified and less dependent on the curvature of the panels. These results are consistent with the conclusions drawn previously, permitting the distinction of three different zones. Considering the inherent limitations of the technique at high frequencies, it is concluded that further improvement is still needed to increase the accuracy of the technique mainly at the very low-frequency range.

IV. MODIFIED TET WITH DOUBLE EXCITATION

In both the original TET and the modified TET using two accelerometers, one of the most important functions of the tip is to transform a force excitation into a moment one. However, by driving the tip, unwanted in-plane force (in the tangential plane for curved panels) and other tip inertia quantities are simultaneously applied. Discussions on the effects of all six inertia forces and moments of the tip have been made using finite element results on an attached panel.[6] Using a selected configuration, the results seemed to indicate that, compared to $M_y(t)$, the other inertia quantities had negligible effects on the system for most frequencies. The transverse motion (in the Z direction) seemed to have a more noticeable influence on the measurements around the resonant values of the system. In fact, in the present configuration, among these quantities, only the in-plane force and the moment $M_y(t)$ are directly related to the excitation, while all others are produced via the tip motion. By neglecting the effects of other inertial forces and moments, the angular displacement θ_y can be regarded as the resultant of two components: θ_m caused by a pure moment excitation and θ_f by the in-plane force excitation:

$$\theta_y = \theta_m + \theta_f . \tag{12}$$

Therefore, the real angular displacement response due to the moment excitation is the difference between the total angular response θ_y and the angular response due to the force excitation θ_f. The rotational compliance should then be

$$(CR)_m = CR - (CR)_f , \tag{13}$$

where $(CR)_m = \theta_m / M_y$ is the rotational compliance to be measured, CR is the rotational compliance estimated as before, and $(CR)_f = \theta_f / M_y$ is the component resulted from the in-plane force excitation.

Equation (13) shows that it is this in-plane force that results in some rotational compliance error, which is more obvious at low frequencies. To eliminate this unfavorable effect, a so-called modified TET with double excitation is used. It consists in applying the modified TET as has been established previously to obtain the total quantity CR. Then, an exciting force is applied at the base of the tip along the tangential direction of the structure where the tip is connected. With the use of two accelerometers already on the tip, one gets the angle response under the in-plane force excitation as follows:

$$\theta_f = (\Delta A_x)_f / h_a \omega^2 , \tag{14}$$

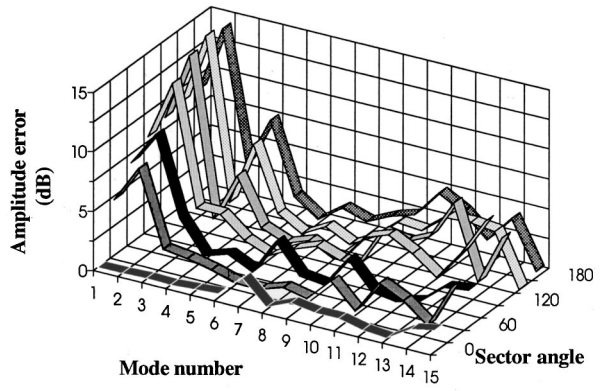

FIG. 10. Comparison of the amplitude error of modal response.

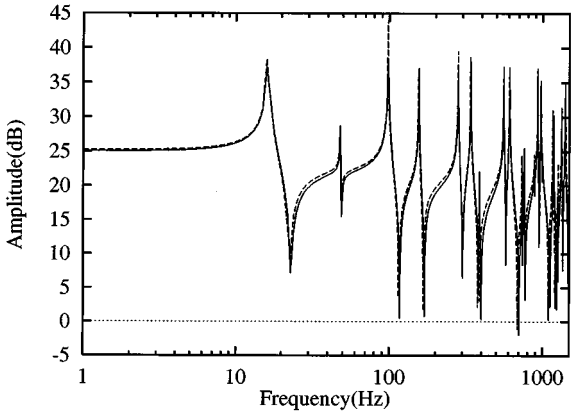

FIG. 11. Comparison of the rotational compliance of the panel with α=30°. Modified TET with double excitation. Expected results: (———); simulated results: (------).

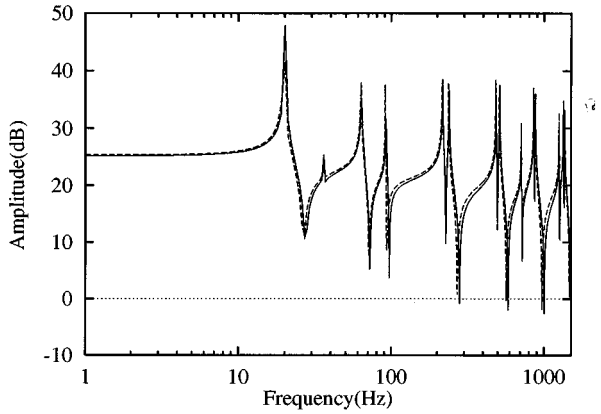

FIG. 12. Comparison of the rotational compliance of the panel with $\alpha=180°$. Modified TET with double excitation. Expected results: (———); simulated results: (------).

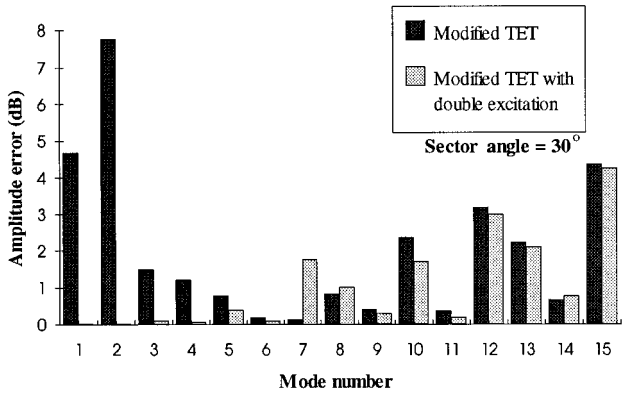

FIG. 13. Amplitude error of modal response for a panel with $\alpha=30°$. Comparison between the modified TET with two accelerometers and the modified TET with double excitation.

in which $(\Delta A_x)_f$ is the same term as defined in Eq. (9) with a subscript f indicating that it is an in-plane force that is applied. By assuming a simple relation between the moment excitation and the exciting force $F(t)$ and neglecting the tip motion, one gets

$$M_y(t)=h_f F(t). \tag{15}$$

$(CR)_f$ can then be estimated by

$$(CR)_f=(\Delta A_x)_f/h_a h_f \omega^2 F_0. \tag{16}$$

Upon obtaining $(CR)_f$, The real rotational compliance of the structure can then be derived from Eq. (13).

Note that it is equally possible to derive a more complete relation instead of Eq. (15) by considering the tip motion since all required quantities are available, resulting in a lengthy expression. However, numerical simulations showed that this treatment was merely necessary since the modifications made aim at low frequencies. It is also important to note that although the technique requires double excitation, it does not mean, however, that the double excitation should be simultaneously applied. As indicated by the technique, two measurements, each one using a single force exciter, can be made quite independently. The results are then made use of to derive the rotational compliance.

The modified TET with double excitation is first validated using numerical simulations on two clamped panels with two sector angles: $\alpha=30°$ and $\alpha=180°$. The obtained results are illustrated, respectively, in Figs. 11 and 12 in terms of compliance amplitude. In both figures we notice a very good agreement between the simulated and expected results. As expected, the modified TET with double excitation seems to completely resolve the problems at low frequencies. No noticeable influences are observed at middle- and high-frequency ranges. To further illustrate the compensation effect, the amplitude errors defined previously were calculated with respect to the results issued from the modified TET and the modified TET with double excitation respectively for 30° and 180° sector angle panels. Again the results were expressed versus the mode number in Figs. 13 and 14, respectively. It can be seen that the compensation effect of the modified TET with double excitation is very effective for the first five modes.

The technique was equally tested using a totally free panel with $\alpha=180°$, which involves more significant rigid motion with respect to the clamped one. The comparison is plotted in Fig. 15 in terms of the compliance amplitude. Again, a very good agreement between the simulated and expected results can be noticed.

V. EXPERIMENTAL STUDY

Experimental measurements were performed to assess the modified TET with double excitation. A free steel semicylindrical shell was used. The panel was 416.6 mm long (unfolded length), 300 mm wide, and 3 mm thick. To simulate a free boundary condition, the curved panel was suspended on a steady base frame with four rubber bands of very weak stiffness at the panel's corners. This suspension method has been proved to be effective to simulate free boundaries.[9] An aluminum tip was fixed with three screws and glued to the panel using high strength fast glue (LEPAGE epoxy syringe). The tip was fixed at a point 5 cm from the corner of the straight edge.

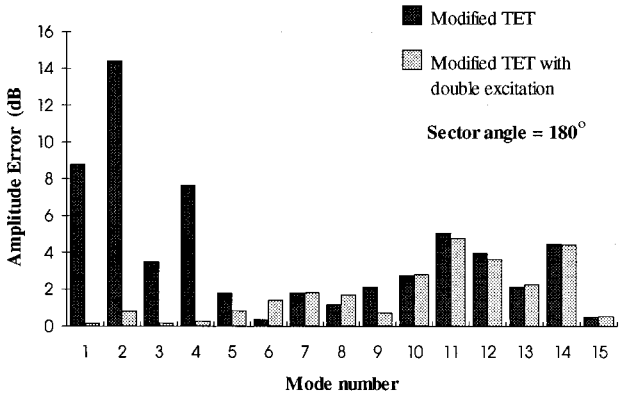

FIG. 14. Amplitude error of modal response for a panel with $\alpha=180°$. Comparison between the modified TET with two accelerometers and the modified TET with double excitation.

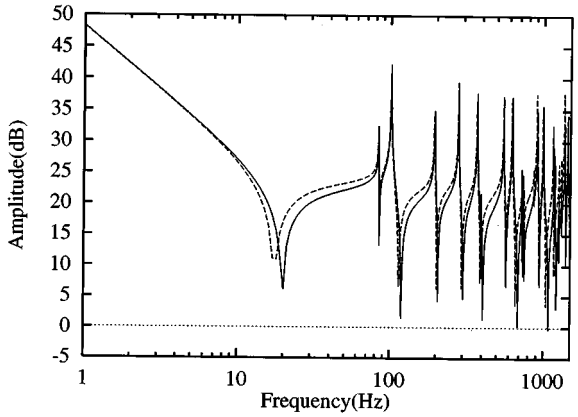

FIG. 15. Comparison of the rotational compliance of the free panel with $\alpha=180°$. Modified TET with double excitation. Expected results: (———); simulated results: (------).

Details about experimental setup and the measurement block diagram were identical to those reported in Ref. 7. Basically, a B&K 2035 signal analyzer was used to generate a random excitation signal. A B&K 4809 vibration exciter was used to apply a excitation force to the test system and the generated forces were measured by a B&K 8200 force transducer. The acceleration response was measured by a tiny B&K 4393 accelerometer installed in the different places on the tip as specified by the technique. Both force and acceleration signals were then analyzed using the B&K 2035 signal analyzer. Measured data were then transferred to a HP work station to make calculations.

The measured compliance curve using the modified TET with double excitation was compared to the expected results in Fig. 16. The first peak appeared in the spectrum corresponded to the first nonzero natural frequency of the panel. The reason that the curve began at 40 Hz was due to the fact that we could not obtain a good signal-to-noise ratio below this frequency. The agreement between the experimental and expected results are generally good. A good coincidence of the resonance peaks can be observed for the whole frequency range used. The amplitude difference is generally within 3 dB except for some antiresonance regions.

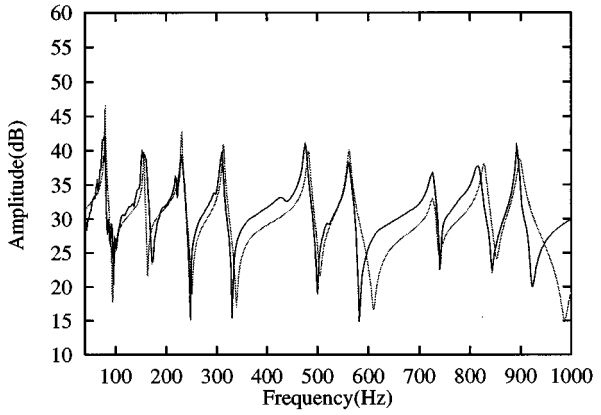

FIG. 16. Comparison of the rotational compliance of the free panel with $\alpha=180°$. Modified TET with double excitation. Experimental results: (———); simulated results: (------).

VI. CONCLUSIONS

As an extension of the previously established tip excitation technique, the present work discussed applications of the TET to curved structures. Three versions of the techniques were proposed and assessed via numerical simulations. Experimental validations were also made using a representative configuration. It was demonstrated that the original TET can provide an acceptable accuracy for rotational compliance only in the middle-frequency range. At low frequencies involving a few structural modes, the accuracy was clearly insufficient due to the inaccurate indication of the rotational response and the effect of the in-plane force excitation. Compared with the original TET, the modified TET using two accelerometers brought an obvious improvement at low frequencies. The advantage of these two versions of the technique is their simplicity, since in both cases, only a single excitation is needed at the top portion of the tip. The third version of the TET requires a two-step measurement. It consists in separately exciting the tip both at the top and on the base and measuring the corresponding acceleration responses. These two tests may be performed separately requiring no synchronization. Both numerical and experimental results showed that the modified TET with double excitation ensures a good estimation accuracy for the rotational compliance for all low- and middle-frequency ranges. From this point of view, it becomes possible to apply the modified TET with double excitation to curved structures to reach the same performance as the original TET does to the plane structures. We believe that the obstacles limiting the application of the TET to curved structures are now removed.

[1] ANSI S2.34-1984, ''American National Standard Guide to the Experimental Determination of Rotational Mobility Properties and the Complex Mobility Matrix'' (American National Standards Institute, New York, 1984).
[2] D. J. Ewins, *Modal Testing: Theory and Practice* (Research Studies Press, Tauton, Somerset, 1984).
[3] H. G. D. Goyder, ''Methods and application of structural modeling from measured structural frequency response data,'' J. Sound Vib. **68**(2), 209–230 (1980).
[4] M. A. Sanderson and C. R. Fredô, ''Direct measurement of moment mobility, Part I: A theoretical study,'' J. Sound Vib. **179**(4), 669–684 (1995).
[5] M. A. Sanderson, ''Direct measurement of moment mobility, Part II: An experimental study,'' J. Sound Vib. **179**(4), 685–696 (1995).
[6] L. Cheng and Y. C. Qu, ''Rotational compliance measurement of a flexible plane structure by means of an attached beamlike tip. Part I: Analysis and numerical simulation,'' to appear in J. Vib. Acoust. Trans. ASME **119** (1997).
[7] Y. C. Qu, L. Cheng, and D. Rancourt, ''Rotational compliance measurement of a flexible plane structure by means of an attached beamlike tip. Part II: Experimental study,'' to appear in J. Vib. Acoust. Trans. ASME **119** (1997).
[8] D. A. Wells, *Theory and Problems of Lagrangian Dynamic* (McGraw-Hill, New York, 1967).
[9] L. Cheng and R. Lapointe, ''Vibration attenuation of panel structures by optimally shaped viscoelastic coating with added weight consideration,'' Thin-Walled Struct. **21**, 307–326 (1995).